Journal of the Royal Society of Western Australia, Vol. 65, Part 2, 1982, p. 69-85.

A layered ultramafic intrusion in Archaean granulites near Lake Kondinin, Western Australia

By W. R. Morgan
12 Hobbs Avenue, Como, W.A. 6152
(formerly Geology Department, Western Australian Institute of Technology)

Manuscript received 18 November 1980; accepted 22 September 1981

Abstract

An ultramafic body is enclosed in felsic and mafic granulites and is composed of lherzolite and harzburgite units. The lherzolite is considered in detail; it consists of 11 cycles, each ranging from olivine-rich to olivine-poor rocks. In one cycle, the olivine-pyroxene rocks are followed successively by hornblende-plagioclase and clinopyroxene-plagioclase rocks. There is considerable Fe-enrichment in the hornblende-rich zone. The lherzolite is a layered body formed by repetitive intrusion, crystal settling, and expulsion of tholeiitic magma under conditions of high-grade metamorphism. The crystallization of Fe-rich hornblende suggests that the body could have been a source of calc-alkaline magma.

Introduction

The effects of high-grade metamorphism on ultramafic rocks have been a matter of some controversy (O'Hara 1961, 1965; Bowes *et al.* 1964). More recently, workers such as Davies (1974) and Windley (1977), in studies of Archaean ultramafics from high-grade metamorphic terrains, have detected relict igneous stratigraphy, layering, and chemistry through a possible metamorphic overprint. Although these complexes appear to have crystallized from hydrous tholeiitic magmas (Windley 1977), precipitation of amphibole and magnetite was largely responsible for the overall calc-alkaline character of many of these intrusions. The present investigation discusses a lherzolite unit in an ultramafic body in the light of these several views.

General geology

The ultramafic complex, of which the lherzolite is a part, is located 3 km north of the Corrigin-Kondinin road, near Lake Kondinin, 217 km east-south-east of Perth, Western Australia (Fig. 1). It occurs in the Archaean Yilgarn Block, which consists of granitoids, high-grade gneisses and schists, and greenstone belts. Work by Prider (1945), Wilson (1971), Wilson and Green (1971), Davidson (1968, 1971), and Davidson and Mathison (1973, 1974) shows that lenticular, often structurally deformed, mafic and ultramafic bodies occur within hypersthenic gneisses in the Dangin-Quairading area, 80 km north-north-west of Lake Kondinin, and the ultramafic complex described here seems to form part of this granulite-facies terrain.

Between Corrigin and Kondinin, the sparsely outcropping felsic gneisses have contorted foliation trending north to north-west with steep easterly and north-easterly dips. The gneisses, which are fine-grained and foliated, contain microcline-perthite, plagioclase, biotite and, in places, hypersthene and cordierite. Mafic gneisses are known only from rubble in wheat paddocks. They contain intermediate plagioclase, two pyroxenes and, commonly, hornblende.

Surface geology of the ultramafic complex is mostly obscured by a salt lake; a few poor outcrops of silicified and ferruginized serpentinite, along with some amphibole-rich peridotite, can be found on the western side of the lake. A simplified map of part of an aeromagnetic survey carried out by the Electrolytic Zinc Co. of Australasia is presented in Figure 1. The reticulate pattern of positive anomalies represents Proterozoic dolerite dykes. The crescent-shaped anomaly is the ultramafic complex, and indicates that it covers an area of 2.5 km by 1 km. The anomaly was drilled by Electrolytic Zinc at the four locations indicated on Figure 1 and details of drill hole depth and orientation are given in Table 1. This paper results from a detailed petrographic examination of the cores with analyses of selected rocks and their minerals from DDH C3, C4, and C5.

Because of the location of the complex beneath the western side of the lake the holes were drilled down the dip of the regional structure. An attempt

Table 1

Diamond drill hole data

Hole No.	Azimuth (magnetic)	Plunge	Depth (metres)
C2	90°	60°	243·84
C3	82°	45°	265·18
C4	90°	45°	231·65
C5	47°	65°	249·02

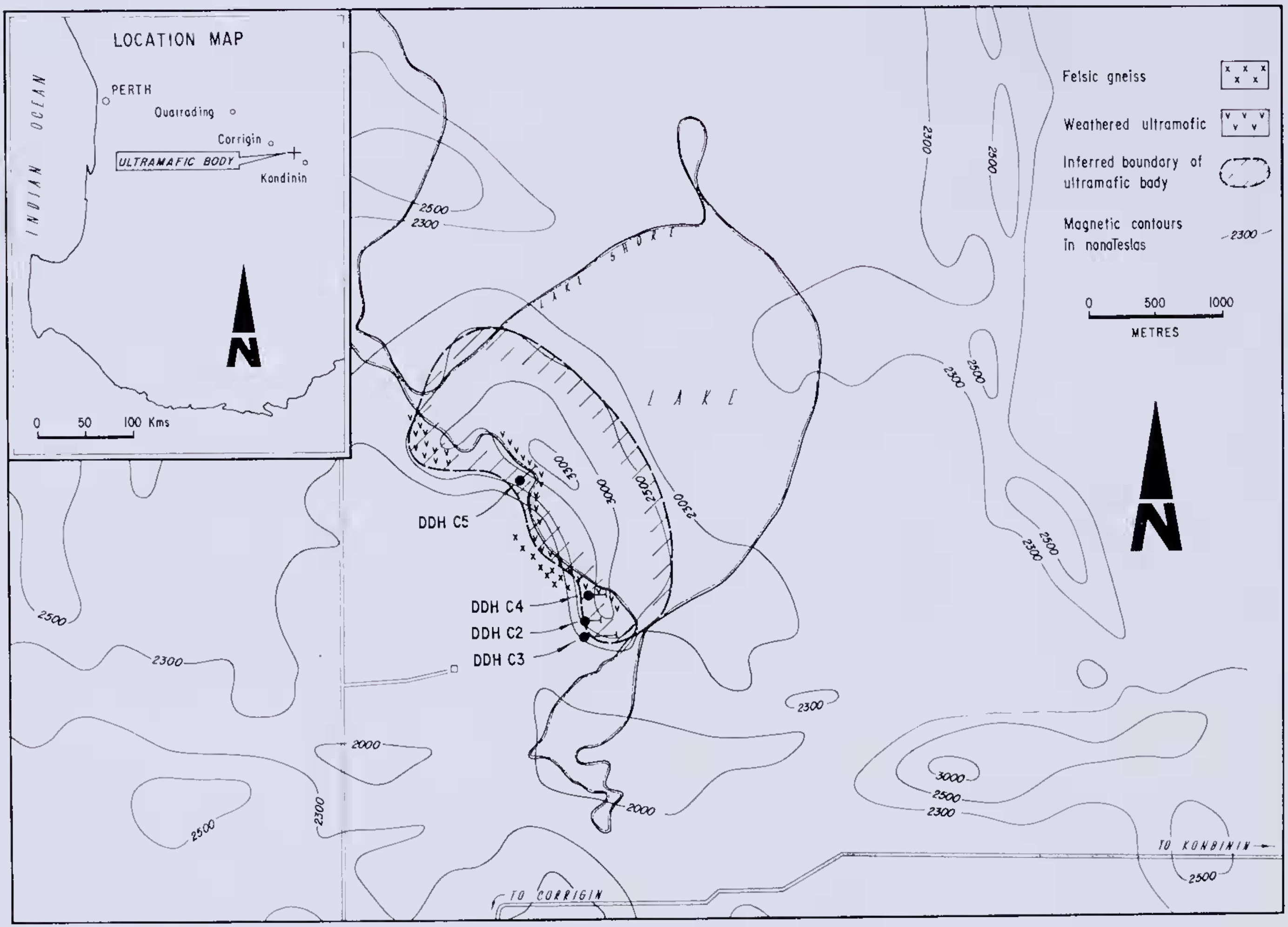

Figure 1—Simplified aeromagnetic anomaly map of the ultramafic near Lake Kondinin. Reproduced by permission of the Electrolytic Zinc Co. of Australasia. Inset: Location map, south Western Australia.

was made to find the angular and azimuthal relation between vague planar structures occasionally seen in the cores and the plunge of the drill holes by the Phillips (1971) method; however, this failed, hence the true thicknesses of the units to be described are not known.

Contact relations between the ultramafic body and the surrounding felsic gneiss—at 63 m in DDH C4 and 36 m in DDH C2—are inconclusive. In C4, weathered gneiss abuts dark ferruginous clay that shows serpentinite-like structures. In C2, the gneiss is in contact with silicified and ferruginized serpentinite. In neither case are there any structures or textures that would suggest a faulted contact, or hornfelsing of the gneiss by the ultramafic.

Harzburgite unit

Investigation of the harzburgite unit is still proceeding; the results will be described in a second paper (Morgan in prep.). Work so far shows it to consist of olivine and orthopyroxene, together with chromiferous magnetite and phlogopite. It is strongly serpentinized, particularly in DDH C3. Texturally, it contains orthopyroxene megacrysts up to 10 cm long enclosed in a matrix of olivine and orthopyroxene with an average grain size of about 2 mm. In DDH C3, the southernmost hole, the megacrysts are euhedral and unstrained. In DDH C4, and particularly the northernmost hole, DDH C5, the megacrysts are increasingly strained, showing mosaic substructure and marginal to complete polygonization. The matrix minerals in all holes are sub-rounded to polygonal and unstrained. Chemical analysis of rocks and minerals suggest that the harzburgite is unlike "depleted" ophiolite and mantle peridotite. The contact of the harzburgite and lherzolite is obscured by a later thin granitic intrusion in DDH C4, and unrecovered core in DDH C5.

Amphibole lherzolite unit

Petrography

Mineral variations.—Variations in the proportions of minerals in the lherzolite suggest a relict igneous layering, the layers ranging between 0.3 and 8 m along the core. The lherzolite unit consists, for the most part, of olivine, orthpyroxene, and tremolite, with subordinate colourless clinopyroxene, magnetite and, rarely, phlogopite. Olivine and sometimes orthopyroxene are slightly to moderately serpentized. In DDH C4 rocks containing hornblende, pale green clinopyroxene and plagioclase are present between 217.48 m and 219.46 m depth.

Modal variations with depth in the lherzolite unit in DDH C4 are shown in Figure 2. The diagram shows a series of repeated layers. In each of the layers there is a gradation from olivine-rich to

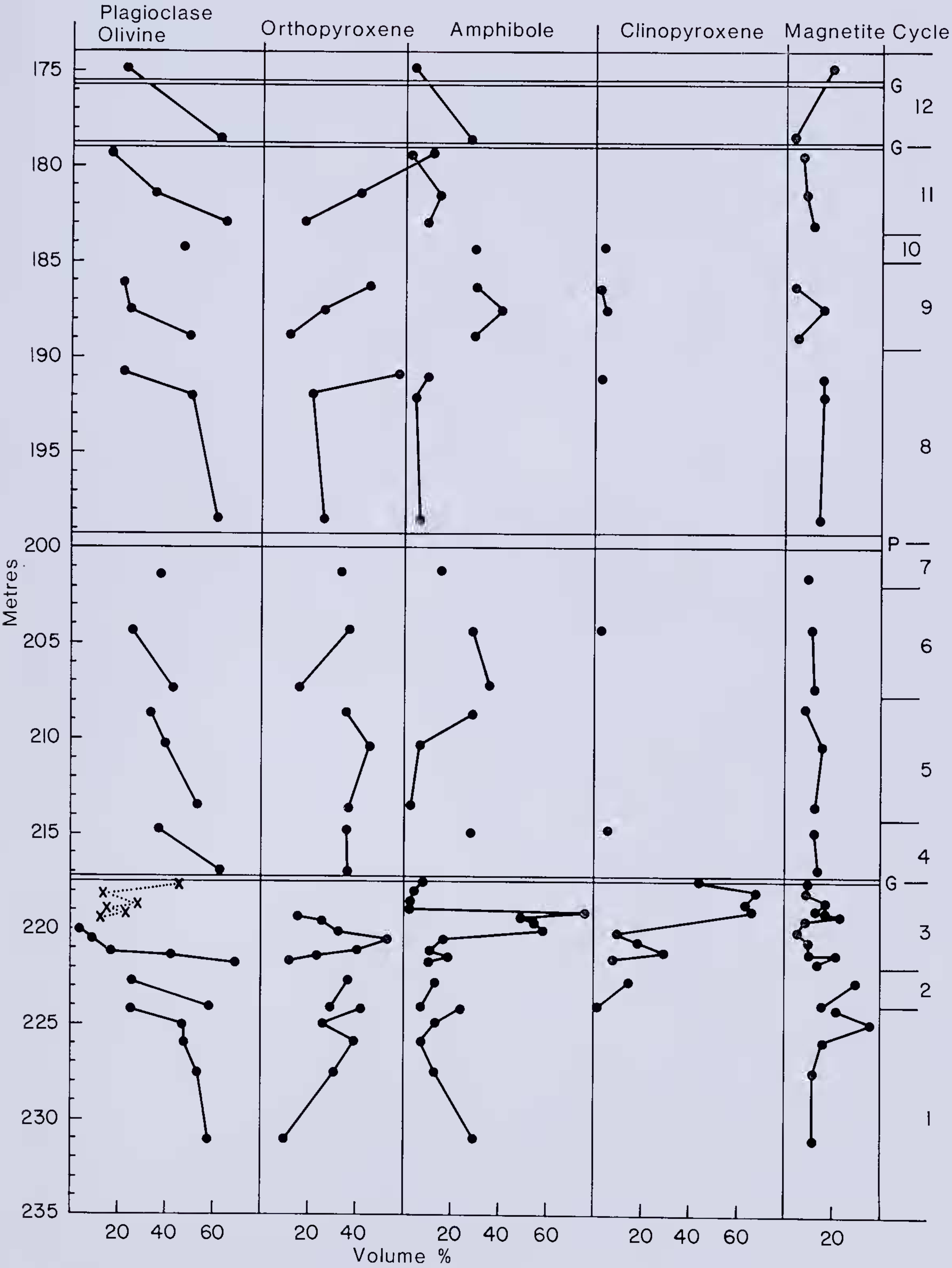

Figure 2.—Modal variations with depth in the lherzolite unit, DDH C4. • = ferromagnesian minerals, X = plagioclase, P = pegmatite, G = acid intrusive.

olivine-poor ultramafic rock. The cycles are not identical; some lead to impoverishment and others to enrichment in lime-bearing minerals. Cycle 3, between 221.74 m and 217.4 m, proceeds from tremolite lherzolite at 221.74 m to tremolite orthopyroxenite at 220.68 m. Next, amphibole increases and changes in composition from tremolite to hornblende until at 219.47-219.30 m the rocks are orthopyroxene hornblendite; at this level, subordinate amounts of plagioclase are present, and there is a moderate increase in magnetite content. At 219.25 m orthopyroxene is absent. Just above this level, at 219.15 m, hornblende is absent, the amount of magnetite is reduced and rocks with pale green clinopyroxene and plagioclase extend up to 217.48. Immediately above this point is a thin, later, biotite adamellite intrusion, followed by olivine-rich rocks of cycle 4.

That the cycles in the drill core are not the result of repetition by folding or faulting is shown by the fact that the decrease in olivine content trends "up" the core in every cycle and because of the significant differences in mineralogy between the cycles (as shown in Fig. 2). Mineralogical variations suggest that this is relict igneous layering.

Textures.—Olivine, orthopyroxene and, where present, clinopyroxene, form polygonal grains ranging from 0.3 to 3 mm diameter. None of the minerals shows straining or kinking. Grain margins are curved or straight. In some rocks olivine has a coarsely amoeboid form. No relict igneous cumulate textures can be seen. Tremolite, in many samples, forms large poikilitic-like plates ranging up to 5 mm across enclosing embayed olivine and orthopyroxene. At first sight this relationship appears to be igneous. However, in other rocks, tremolite is euhedral against olivine and orthopyroxene; some tremolite, indeed, forms fibrous crystals growing into olivine. Commonly, where tremolite encloses clinopyroxene, there is a ragged margin between the two suggesting a reaction relationship with clinopyroxene the primary mineral. The textures as a whole, therefore, are metamorphic. In the hornblende-plagioclase and clinopyroxene-plagioclase rocks of cycle 3 the constituent minerals form polygonal grains with near-straight margins and triple junctions.

Chemistry.—Samples were analysed from cycles 1, 2, 3 and 9 in order to examine the mineralogical trends noted from the modal analyses. The chemical analyses and norms are shown in Table 2. Except for some calcic melanocratic gabbro in cycle 3 all rocks are normatively ultramafic.

In the lherzolite Fe/Mg ratios are higher than in alpine-type ultramafics, demonstrating that the body is not a slice of ophiolite but chemically more similar to cumulate rocks in layered intrusions. All the lherzolites are low in Al_2O_3. For the most part, CaO/Al_2O_3 ratios are greater than 1, hence they do not seem to be komatiitic rocks (e.g. Nesbit and Sun 1976; Morgan 1977) as is shown in Figure 3. The lherzolites, the hornblendic and the plagioclase-clinopyroxene rocks show little correspondence with the Archaean tholeiitic, komatiitic or calc-alkaline series (Fig. 3).

Variation of elements with depth is shown in Figure 4. The ultramafic rocks in each cycle are similar, except for slight differences in the behaviour of Ca, Si and Fe. Rocks above the lherzolite zone of cycle 3 show curious features, particularly in the interval between 220.17 m and 219.25 m where plagioclase and amphibole are present. Here, Si, Mg, Cr and Ni decrease, and $Fe^{+2}/(Fe^{+2} + Mg)$, Fe^{+3}, Al and Ti increase. Above 219.25 m, in the clinopyroxene-plagioclase rocks, Si and particularly Ca increase, $Fe^{+2}/(Fe^{+2} + Mg)$ and Fe^{+3} decrease, and other elements remain more or less constant.

Although cycle 3 gives the impression of a series of rocks in a cumulative differentiation sequence, the $Fe^{+2}/(Fe^{+2} + Mg)$ ratios, the enrichment in Ca and Al, and the decrease in Si are unusual. One could conclude that the hornblende-rich zone between 220.07 m and 219.25 m resulted from reaction between the ultramafic rock below and the clinopyroxene-plagioclase rock above during the metamorphism. A similar situation was described by O'Hara (1961) from the Scottish Lewisian, where elemental variation across the contact from dunite peridotite to garnetiferous basic gneiss is similar to that described in this report. At Kondinin, several factors argue against this interpretation. Firstly, a hornblendic zone is not seen *above* the clinopyroxene-plagioclase rock, at the top of which is a one-metre wide adamellite intrusion; above the adamellite is the olivine-rich base of cycle 4 with no sign of a hornblende-rich zone. Secondly, is the general cyclic nature of the lherzolite—all cycles trend "up" the core. Thirdly (following from the second point) is the clinopyroxene-plagioclase rock, with over 20% CaO (Table 2); it is far too calcic to be a metagabbro and must, itself, have been a cumulative rock of clinopyroxene and, perhaps, plagioclase thus continuing the cumulative sequence of cycle 3.

The iron-enriched, silica-poor hornblendic zone between 220.07 m and 219.25 m probably represents a cumulative horizon possibly where hornblende crystallized as a cumulative phase. This point will be discussed further.

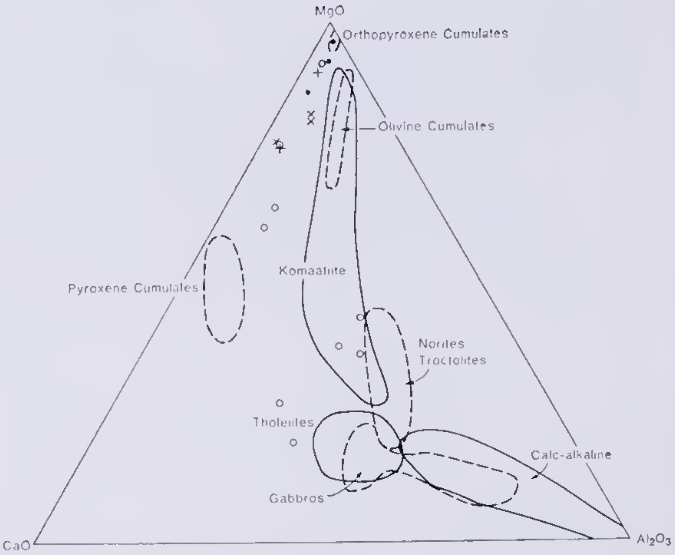

Figure 3.—Plot of MgO-CaO-Al_2O_3 in Archaean tholeiite, komatiite, and calc-alkali suites in relation to the Kondinin rocks: modified from Morgan (1977). Data from Anhaeusser (1971), Donaldson (1974), Hallberg (1972), Hallberg *et al.* (1976 a and b), Hallberg & Williams (1972), Jaques (1976), McCall & Leishman (1971), McIver (1975), Naldrett & Mason (1968), Nesbitt (1971), Purvis, *et al.* (1972), Pyke, *et al.* (1973), Viljoen & Viljoen (1971), White, *et al.* (1971), Williams & Hallberg (1973), Wilson, *et al.* (1969).

Table 2

Analyses and norms of the lherzolites and associated rocks from DDH C4

	Cycle 1			Cycle 2		Cycle 3											Cycle 9		
Depth in metres	225·86	224·94	224·33	224·18	222·81	221·74	221·29	220·68	220·09	220·07	219·46	219·30	219·25	219·51	218·08	217·48	188·67	187·45	186·08
SiO_2	41·95	36·39	43·29	40·91	44·31	40·25	49·94	50·84	51·88	51·70	40·77	40·44	40·34	44·39	48·49	44·32	44·22	46·78	48·04
TiO_2	0·14	0·18	0·14	0·11	0·17	0·13	0·13	0·14	0·19	0·36	0·83	0·82	0·92	0·77	0·39	0·87	0·17	0·20	0·25
Al_2O_3	0·84	0·92	0·99	0·93	1·31	0·96	0·84	1·24	2·71	2·97	11·89	13·39	12·00	12·17	8·50	14·74	2·06	0·68	1·69
Fe_2O_3	7·82	14·51	9·08	7·77	10·28	8·51	7·28	4·90	2·97	1·30	10·37	10·25	10·81	5·12	2·69	5·21	6·68	6·79	5·88
Cr_2O_3	0·65	0·64	0·55	0·58	0·51	0·61	N.D.	0·56	0·65	0·02	0·02	0·02	0·02	0·02	N.D.	0·01	0·46	0·56	0·45
FeO ...	9·48	12·67	10·10	10·51	10·05	10·02	7·36	8·62	7·14	7·37	9·79	8·97	7·88	6·77	4·89	4·84	7·02	6·16	7·59
MnO	0·32	0·29	0·32	0·33	0·29	0·34	0·24	0·26	0·25	0·31	0·44	0·39	0·36	0·33	0·36	0·31	0·26	0·31	0·29
MgO	33·19	29·73	28·47	32·13	24·56	32·62	25·28	24·97	21·88	22·10	15·02	12·97	13·92	9·12	12·28	8·39	29·71	28·46	28·11
NiO	0·17	0·19	0·16	0·18	0·15	0·22	N.D.	0·15	0·14	0·06	0·02	0·02	0·01	0·02	N.D.	0·01	0·19	0·16	0·13
CaO	0·52	1·55	3·47	2·48	6·54	1·80	7·31	6·65	9·36	11·28	8·10	9·78	11·11	20·36	20·69	20·26	4·87	7·71	4·33
Na_2O	0·04	0·05	0·05	0·06	0·12	0·18	0·06	0·12	0·29	0·23	0·67	0·74	0·78	0·19	0·20	0·32	0·26	0·17	0·18
K_2O	0·03	0·02	0·03	0·03	0·08	0·21	0·03	0·05	0·10	0·11	0·18	0·23	0·27	0·05	0·14	0·06	0·55	0·04	0·39
P_2O_5	0·003	0·002	0·002	0·003	0·002	0·005	N.D.	0·007	0·003	0·017	0·009	0·088	0·04	0·04	N.D.	0·06	0·01	0·02	0·01
Loss	4·93	2·39	3·03	4·09	1·79	4·39	1·09	1·37	1·90	1·60	1·60	1·71	1·38	0·85	1·18	0·41	3·29	1·42	2·13
Total	100·08	99·53	99·68	100·11	100·16	100·24	99·56	99·88	99·47	99·43	99·87	99·82	99·84	100·20	99·81	99·81	99·74	99·46	99·47
Ba	N.D.	N.D.	N.D.	N .D.	N.D.	100	N.D.	100	100	240	220	100	100	100	N.D.	100	N.D.	N.D.	N.D.,
Co	276	352	241	280	222	280	N.D.	166	106	98	212	157	231	48	N.D.	108	218	130	196
Cr	4 460	4 386	3 742	3 962	3 492	4 156	N.D.	3 850	4 445	138	136	143	100	166	N.D.	60	3 135	3 800	3 084
Ni	1 330	1 500	1 280	1 400	1 180	1 700	N.D.	1 180	1 130	458	138	132	80	120	N.D.	80	1 460	1 255	1 000
V	41	106	67	49	102	47	N.D.	57	71	94	261	246	N.D.	234	N.D.	N.D.	49	N.D.	58
Zn	45	80	80	135	105	80	N.D.	135	95	70	110	85	84	40	N.D.	30	110	85	70
qz	....	....	....	....	....	....	0·02	....	1·12	....	....	....	....	....	....	....	....	....	....
le	....	....	....	....	....	....	....	....	....	....	....	....	....	0·22	....	0·26	....	....	....
ne	....	....	....	....	....	....	....	....	....	....	....	....	....	0·88	....	1·48	....	....	....
or	0·17	0·11	0·17	0·17	0·45	1·22	0·17	0·28	0·61	0·67	1·06	1·34	1·61	....	0·83	....	3·23	0·22	2·28
ab ...	0·37	0·42	0·42	0·52	1·00	1·52	0·52	1·00	2·46	1·94	5·66	6·24	6·61	...	1·68	....	2·20	1·42	1·52
an	2·00	2·23	2·39	2·17	2·84	1·20	1·92	2·73	5·79	6·73	28·90	32·54	28·43	32·21	21·89	38·61	2·84	1·00	2·67
di wo	0·24	2·28	6·19	4·23	12·36	3·22	14·34	12·61	16·97	20·51	4·68	6·43	11·02	26·74	33·70	25·35	8·87	15·52	7·83
di en	0·19	1·77	4·79	2·91	9·49	2·51	11·33	9·53	12·79	15·11	3·43	4·73	8·64	18·42	24·92	19·28	7·12	12·63	6·16
di fs	0·03	0·28	0·75	0·53	1·56	0·36	1·40	1·81	2·45	3·44	0·82	1·08	1·17	6·17	5·53	3·46	0·73	1·02	0·79
en en	29·65	25·67	39·61	27·90	35·43	25·39	51·62	51·69	41·70	33·53	19·53	13·88	7·48	....	1·40	....	26·81	33·59	46·49
en fs ...	4·36	3·90	6·27	4·56	5·82	3·65	6·33	9·83	8·03	7·64	4·54	3·15	1·03		0·32	....	2·73	2·73	6·00
ol fo	40·17	32·66	18·57	34·49	11·38	37·38	....	0·69	....	4·49	10·12	9·60	13·00	2·91	2·98	1·13	28·07	17·28	12·17
ol fa	5·37	5·48	3·24	6·21	2·06	5·91	....	0·14	....	1·14	2·61	2·45	1·94	1·08	0·73	0·22	3·14	1·55	1·73
il	0·27	0·35	0·27	0·21	0·32	0·24	0·24	0·27	0·36	0·68	1·76	1·56	1·75	1·46	0·74	1·65	0·32	0·38	0·47
mt	11·35	21·05	13·18	11·28	14·91	12·34	10·56	7·11	4·31	1·88	15·03	14·87	15·68	7·43	3·91	7·55	9·68	9·84	8·52
ct	0·96	0·94	0·81	0·85	0·76	0·90	....	0·83	0·96	0·02	0·02	0·02	0·02	0·02	....	0·02	0·67	0·83	0·67
ap	....	....	....	....	....	0·01	....	0·02	....	0·03	0·02	0·02	0·10	0·10	....	0·14	0·02	0·03	0·02
ak	....	....	....	....	....	....	....	....	....	....	....	....	....	1·62	....	0·41	....	....	....
Loss	4·93	2·93	3·03	4·09	1·79	4·39	1·09	1·37	1·90	1·60	1·60	1·71	1·38	0·85	1·08	0·41	3·29	1·42	2·13
Total	100·06	99·53	99·69	100·12	100·17	100·24	99·54	99·91	99·45	99·41	99·78	99·80	99·86	100·11	99·81	99·97	99·72	99·46	99·45

All except FeO determined by XRF.
FeO determined by titration, with subsequent adjustment of Fe_2O_3.
Analysts: Major elements, Cr, V, Ni: General Superintendence, Perth. W.A.
Ba, Co, Zn: W. R. Morgan, Department of Geology, King's College, London.

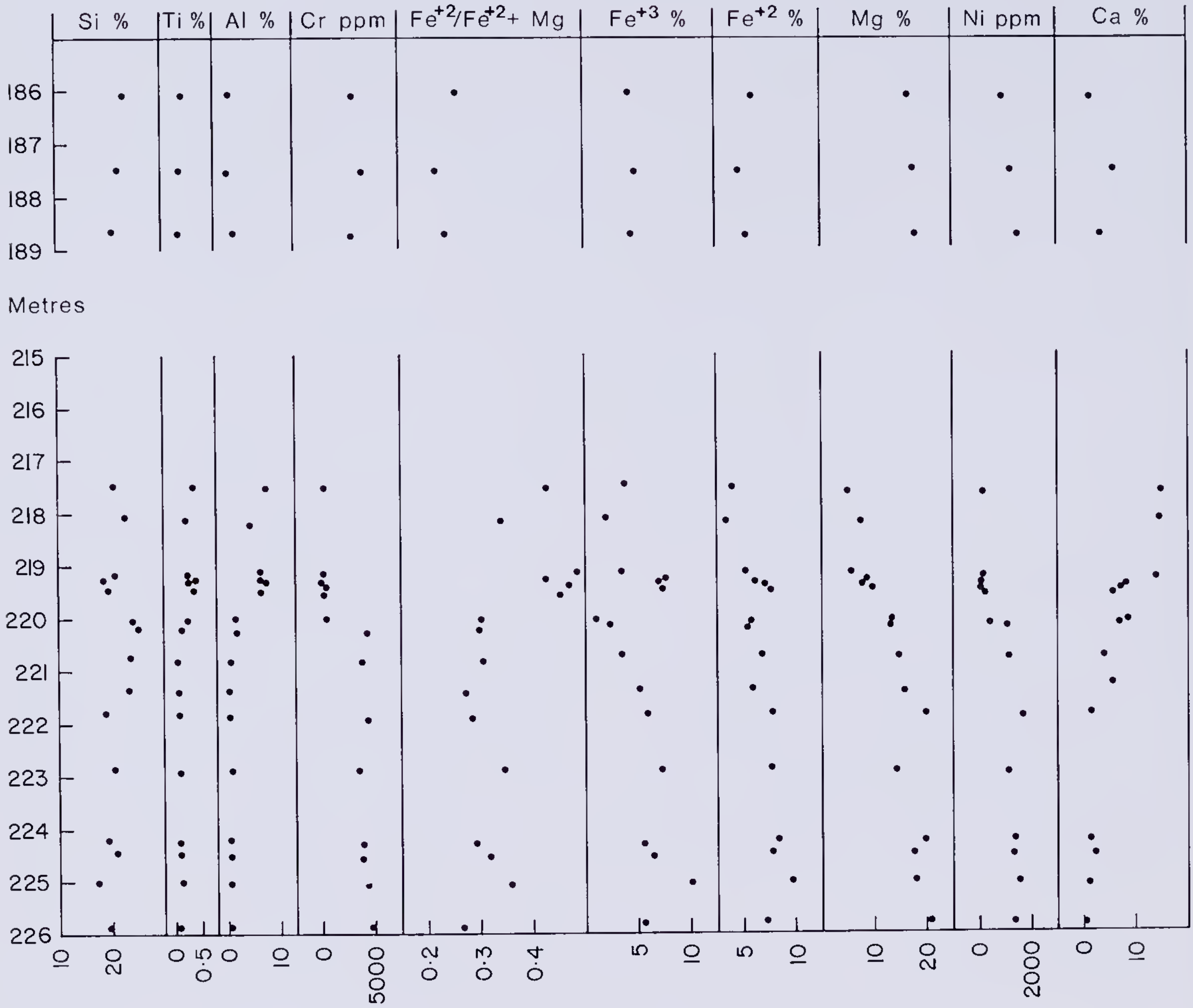

Figure 4.—Variation of elements with depth, DDH C4.

The recast analyses are plotted on the ACF diagram (Fig. 5). They seem to best fit amphibolite granulite-to-transitional facies. The presence in the ultramafic rock of tremolite in preference to clinopyroxene (which tends to occur as relics) and of the assemblage hornblende-plagioclase (though with minor orthopyroxene) supports this view. The presence, in the ultramafic rocks, of hypersthene rather than anthophyllite supports a transition to the granulite facies. However, outcropping on the lake shore are xenolithic inclusions enclosed in ultramafic rock composed of plagioclase, hedenbergite and andradite. The presence of andradite would suggest that the xenoliths, and therefore the ultramafic rock, equilibrated under amphibolite facies conditions (Winkler 1967).

Mineral Chemistry.—Electron micoprobe analyses of olivine, orthopyroxene, clinopyroxene, amphibole, magnetite and plagioclase are presented in Tables 3 to 8. All analyses were carried out by the author on the Western Australian Institute of Technology Seimens Etec Microprobe Analyser, using an accelerating voltage of 20 kV, specimen current of 0.25 x 10^{-7} amps and a 1-2 μm beam diameter. X-ray intensities were converted to oxide percentages using the Magic IV programme.

The Mg/(Mg + Fe) ratios of *olivine* (Table 3) range between 0.845 and 0.889; these values are lower than those of olivine from "depleted" alpine peridotite and peridotite nodules and close to those of cumulate rock in layered intrusion (Green 1964; Frost 1975; Boyd *et al.* 1976). The Fe/Mg ratios vary from cycle to cycle, being lowest in cycle 1 (0.125 - 0.143) and highest in cycle 2 (0.169 - 0.183). Fe-enrichment increases "up" the core in cycles 1 and 2, in agreement with the direction of modal olivine depletion.

The distribution of Mg and Fe between olivine and co-existing orthopyroxene is somewhat variable (Table 9). In cycle 1, the olivine is more Mg-rich than orthopyroxene, with values of K_D [=(Fe/Mg opx)/(Fe/Mg ol)] of 1.1 to 1.2. In other cycles, these values are lower, ranging from between 0.9 and 1.0. However, the K_D values are close to those of Frost

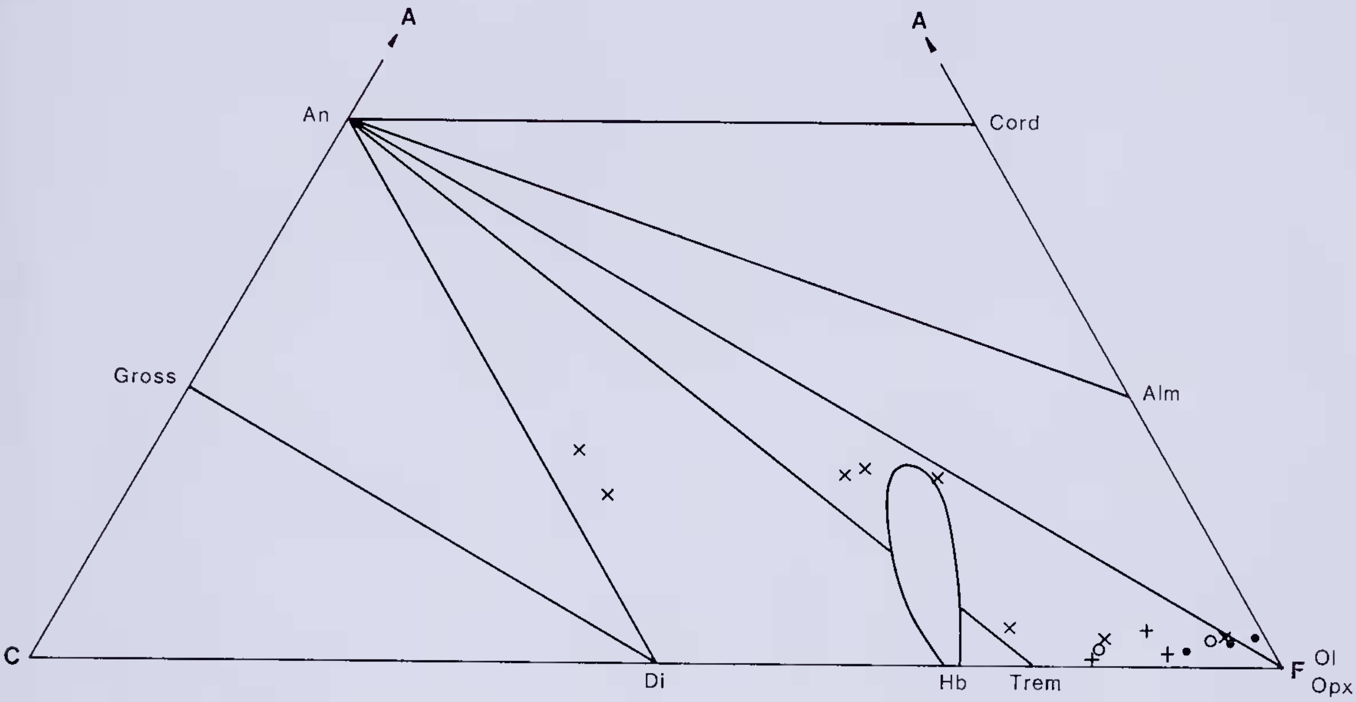

Figure 5.—Plot of Kondinin rocks on A-C-F diagram. Symbols: • cycle 1, o cycle 2, x cycle 3, + cycle 9.

Table 3

Electron microprobe analyses and unit cell contents of olivine in samples selected from DDH C4

	Cycle 1			Cycle 2		Cycle 3	Cycle 9		
Depth in metres	226·86	224·94	224·33	224·18	228·81	221·74	188·67	187·45	186·08
SiO_2	40·22	40·28	40·32	39·35	39·80	40·50	41·51	39·68	40·32
TiO_2	0·01	N.D.	0·01	0·03	0·01	N.D.	0·03	0·01	0·02
Al_2O_3	0·60	0·05	0·58	0·26	0·12	0·04	0·11	N.D.	0·05
Cr_2O_3	0·02	N.D.	0·03	0·04	0·04	0·04	0·01	0·01	0·02
*FeO	10·78	11·44	11·90	13·71	14·71	13·35	12·02	12·14	11·76
MnO	0·45	0·44	0·42	0·49	0·53	0·47	0·41	0·45	0·43
Nio	0·28	0·30	0·31	0·31	0·33	0·27	0·42	0·44	0·41
MgO	48·38	48·44	46·88	45·70	45·12	45·22	45·67	46·54	47·37
CaO	0·03	0·02	0·01	0·03	0·02	0·11	0·01	N.D.	0·02
Na_2O	0·15	N.D.	N.D.	N.D.	0·05	N.D.	N.D.	N.D.	N.D.
K_2O	N.D.	0·01	N.D.	N.D.	N.D.	N.D.	N.D.	N.D.	N.D.
Total	100·92	100·98	100·46	99·92	100·73	100·00	100·19	99·27	100·40
Number of ions on the basis of 4 oxygens									
Si	·984	·989	·955	·987	·994	1·100	1·025	·994	·996
Al	·017	·002	·017	·008	·004	....	·003	....	·002
Ti	Tr.	....	Tr.	·001	Tr.	·001	·001	Tr.	·002
Fe	·221	·235	·246	·288	·307	·277	·248	·255	·243
Cr	Tr.	....	·001	·001	·001	·001	Tr.	Tr.	Tr.
Mn	·009	·009	·009	·010	·011	·010	·009	·010	·009
Ni	·006	·006	·006	·006	·007	·005	·008	·009	·008
Mg	1·765	1·771	1·724	1·708	1·679	1·681	1·680	1·738	1·744
Ca	·001	·001	Tr.	·001	·001	·003	Tr.	....	·001
Na	·007	....	....	....	·002	....	....	....	....
K	...	Tr.	...	....	....	....	..	....	....
Mg	88·9	88·3	87·5	85·6	84·6	85·9	87·1	87·2	87·8
Fe	11·1	11·7	12·5	14·4	15·5	14·1	12·9	12·8	12·2
Mg/(Mg + Fe)	·889	·883	·875	·856	·845	·858	·871	·872	·878
Fe/(Fe + Mg)	·111	·117	·125	·144	·155	·141	·129	·128	·122
Fe/Mg	·125	·133	·143	·169	·183	·165	·148	·147	·139

*All iron as FeO. Analyst: W. R. Morgan, W.A.I.T.

(1975), Challis (1965), Green (1964), and other workers. Of the minor elements, Ni is, as expected, concentrated in olivine. Ti, Al, Cr and alkalies are very low.

Analyses of *orthopyroxene* and *clinopyroxene* are shown in Tables 4 and 5, respectively. Both pyroxenes contain only minor quantities of Cr, Ti, Ni and alkalies. Ti rises to around 0.5% in the more iron-rich clinopyroxene of Cycle 3. Ni reaches 0.22% in the orthopyroxene at 220.68 m. This is presumably because the rock contains as much as 1 180 ppm of Ni (Table 2) but no olivine present to accommodate it. Ni is more evenly distributed between the pyroxenes of the olivine-free rock at 220.09 m.

The lherzolite, and the pyroxenes it contains, are all poor in $Al_2 0_3$. However, $Al_2 0_3$ increases in the higher rocks of cycle 3 reaching 4.33% in the orthopyroxene at 219.3 m. and 3.77% in the clinopyroxene at 217.48 m.

The clinopyroxene of cycle 3, and the orthopyroxene of cycles 1, 2 and 3 show increasing Fe/Mg ratios "up" the core. However, Fe/Mg in orthopyroxene does not vary significantly from cycle to cycle, as in the olivines.

The pyroxenes, particularly the four pairs of coexisting pyroxenes, are rich in Mg with molecular values ranging between 0.911 - 1.042 (clinopyroxene) and 1.623 - 1.730 (orthopyroxene). Hence a direct comparison of these pairs with those of Quairading, Western Australia (Davidson 1968) and Broken Hill, New South Wales (Binns 1962) cannot be made as can be seen from Figure 6. On this diagram, the "higher grade" and "lower grade" granulite facies curves of the Broken Hill and Quairading pyroxenes show clearly their converging increase in K_D [=(Fe/Mg opx)/(Fe/Mg cpx)] with decreasing total iron content (the K_D values were recalculated from Binns' and Davidson's work using total iron, to facilitate comparison with the Kondinin pyroxenes). The Kondinin pyroxenes plot just on the "higher grade" side of the curves close to their origin. If there is any significance in this, bearing in mind the closeness of the curves and the limits of analytical accuracy, it may represent the imprint of an original (igneous) high temperature equilibrium state retained in spite of later metamorphism. Pyroxene, amphibole and olivine, are plotted on the pyroxene quadrilateral of Figure 7. Clinopyroxene is irregularly distributed, plotting over the range of the "higher" and "lower" grade pyroxenes of Broken

Table 4

Electron microprobe analyses and unit cell contents of orthopyroxene in samples selected from DDH C4

	Cycle 1			Cycle 2		Cycle 3					Cycle 9		
Depth in metres	225·86	224·94	224·33	224·18	222·81	221·74	220·68	220·09	219·46	21·930	188·67	187·45	186·08
SiO_2	57·09	57·23	58·32	57·03	57·32	57·10	56·49	55·40	54·00	53·39	57·22	57·35	57·39
TiO_2	0·01	0·05	0·04	0·05	0·05	0·08	0·02	0·06	0·11	0·11	0·07	0·04	0·07
Al_2O_3	0·51	0·97	0·28	0·69	0·69	0·53	0·68	1·23	3·28	4·32	0·48	0·58	0·19
Cr_2O_3	0·08	0·05	0·04	0·03	0·03	0·11	0·10	0·17	0·13	0·03	0·11	0·12	0·04
*FeO	8·52	8·85	9·20	9·26	9·62	8·96	11·11	11·51	13·59	13·52	8·32	8·02	8·47
MnO	0·42	0·44	0·53	0·50	0·52	0·50	0·38	0·50	0·85	0·97	0·51	0·60	0·46
NiO	0·07	0·12	0·06	0·07	0·06	0·08	0·22	0·11	0·04	0·05	0·11	0·11	0·14
MgO	34·01	32·18	30·45	32·53	31·94	32·33	31·09	31·04	28·41	28·28	32·43	33·36	33·55
CaO	0·20	0·71	0·56	0·66	0·64	0·68	0·73	0·61	0·44	0·19	0·61	0·63	0·49
Na_2O	N.D.	N.D.	0·07	0·04	N.D.	N.D.	0·11	N.D.	0·04	0·09	0·06	0·05	N.D.
K_2O	N.D.	N.D.	N.D.	N.D.	0·01	N.D.	N.D.	N.D.	0·01	N.D.	N.D.	0·03	0·02
Total	100·91	100·60	99·55	100·86	100·88	100·27	100·93	100·63	100·90	100·95	99·92	100·89	100·82

Number of ions on the basis of 6 oxygens

Si	1·973	1·986	2·041	1·980	1·990	1·989	1·978	1·952	1·916	1·893	1·996	1·981	1·986
Al^{iv}	·021	·014	....	·020	·010	·011	·022	·048	·084	·107	·004	·019	·008
Al^{vi}	....	·026	·012	·008	·018	·011	·006	·003	·053	·074	·016	·005	
Ti	·0003	·001	·001	·001	·001	·002	·001	·002	·003	·003	·002	·001	·002
Fe	·246	·257	·269	·269	·279	·261	·325	·339	·403	·401	·243	·232	·245
Cr	·002	·001	·001	·001	·001	·003	·003	·005	·004	·001	·003	·003	·001
Mn	·012	·013	·016	·015	·015	·015	·011	·015	·026	·029	·015	·018	·014
Ni	·002	·003	·002	·002	·002	·002	·006	·003	·001	·001	·003	·003	·004
Mg....	1·752	1·664	1·587	1·683	1·653	1·678	1·623	1·630	1·502	1·494	1·686	1·717	1·730
Ca	·008	·027	·021	·025	·024	·025	·027	·023	·017	·007	·023	·023	·018
Na	....	....	·005	·003	....	....	·008	....	·003	·006	·004	·003	....
K	....	....	....	....	Tr.	....	....	....	Tr.	....	....	·001	·001
Mg	87·3	85·4	84·6	85·1	84·5	85·4	82·2	81·8	78·2	78·6	86·4	87·1	86·8
Fe	12·3	13·2	14·3	13·6	14·3	13·3	16·5	17·0	21·0	21·1	12·5	11·8	12·3
Ca	0·4	1·4	1·1	1·3	1·2	1·3	1·4	1·2	0·9	0·3	1·1	1·1	0·9
Mg/(Mg + Fe)	·887	·866	·855	·862	·856	·865	·833	·841	·788	·788	·874	·881	·876
Fe/(Fe + Mg)	·123	·134	·145	·138	·144	·135	·167	·172	·211	·212	·126	·119	·124
Fe/Mg	·140	·155	·170	·160	·169	·156	·200	·208	·268	·268	·144	·135	·142

*All iron as FeO. Analyst: W. R. Morgan, W.A.I.T.

Table 5

Electron microprobe analyses and unit cell contents of clinopyroxene in samples selected from DDH C4

	Cycle 2	Cycle 3				Cycle 9
Depth in metres	222·81	220·68	220·09	218·08	217·48	186·08
SiO_2	53·41	53·64	53·08	50·82	50·00	53·26
TiO_2	0·08	0·11	0·49	0·51	0·31	0·15
Al_2O_3	1·02	1·17	1·04	3·52	3·77	0·97
Cr_2O_3	0·07	0·17	0·16	0·02	0·04	0·19
FeO*	3·22	3·94	4·28	7·10	7·18	3·08
MnO	0·16	0·19	0·29	0·53	0·62	0·20
NiO	0·12	0·11	0·16	N.D.	0·04	0·10
MgO	17·45	17·07	16·52	13·39	14·05	19·27
CaO	23·52	24·20	23·07	23·58	23·27	23·33
Na_2O	0·10	0·26	N.D.	0·44	0·33	N.D.
K_2O	N.D.	0·01	N.D.	N.D.	N.D.	N.D.
Total	99·15	100·87	99·09	99·91	99·61	100·55
Number of ions on the basis of 6 oxygens						
Si	1·965	1·952	1·963	1·898	1·876	1·933
Al^{iv}	·035	·048	·037	·102	·124	·041
Al^{vi}	·009	·002	·008	·053	·043	....
Ti	·002	·003	·014	·014	·009	·006
Fe	·099	·120	·133	·222	·225	·094
Cr	·002	·005	·005	·001	·001	·006
Mn	·005	·006	·009	·017	·020	·006
Ni	·003	·003	·005	....	·001	·003
Mg	·957	·926	·911	·745	·786	1·042
Ca	·927	·943	·914	·944	·935	·907
Na	·007	·018	....	·032	·024	....
K	....	·0004	....	....	....	....
Mg	48·3	46·4	46·5	38·6	40·0	51·0
Fe	5·0	6·6	6·8	12·4	12·5	4·6
Ca	46·7	47·4	46·7	49·0	47·6	44·4
Mg/(Mg+Fe)	·906	·902	·873	·770	·777	·916
Fe/(Fe+Mg)	·094	·114	·127	·229	·223	·083
Fe/Mg	·103	·130	·146	·298	·286	·090

* All iron as FeO. Analyst: W. R. Morgan, W.A.I.T.

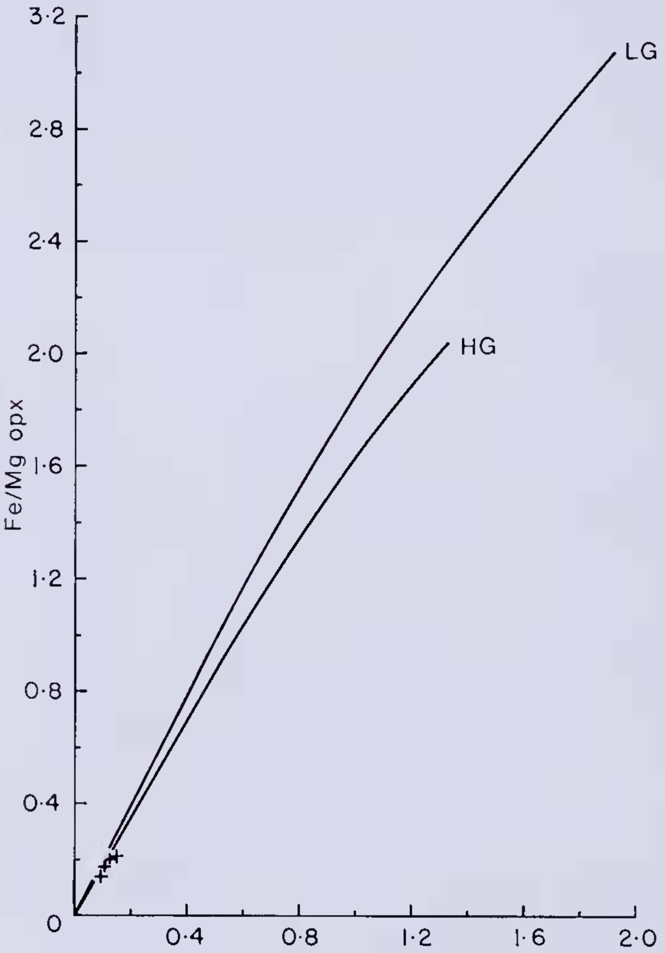

Figure 6.—Graphical solution of K_D [=(Fe/Mg opx)/(Fe/Mg cpx)]. Full lines indicate "higher" and "lower" grade pyroxenes of Quairading and Broken Hill. Crosses are the Kondinin rocks.

Hill and Quairading. Again, perhaps this indicates partial re-equilibration from a higher to a lower temperature environment.

Amphibole analyses are presented in Table 6. In cycle 3, Fe/Mg ratios increase from the lherzolite to the plagioclase-bearing rocks. In other cycles the ratios are less regular unlike those of the olivine and orthopyroxene. Similarly K_D [=(Fe/Mg opx)/(Fe/Mg amph)] and K_D [=(Fe/Mg ol)/(Fe/Mg amph)] are less regular than those for olivine and pyroxenes (Table 9), and this may be due to the late crystallization/recrystallization of amphibole in lherzolite. Textural relationships suggest that it partly replaces clinopyroxene and olivine. Hence the irregular Fe/Mg ratio and K_D values probably indicate disequilibrium.

In cycle 3 however, as hornblende succeeds tremolite the amphibole Fe/Mg ratios rise considerably, more than in the co-existing orthopyroxene and clinopyroxene (Fig. 8; see also Fig. 7). At 219.46 m and 219.3 m the rocks consist largely of hornblende and the rocks themselves have high Fe/Mg ratios.

The amounts of the minor constituents Ti, Cr and Mn, though low, differ from cycle to cycle confirming that the cycles are real and not structurally repeated. The alkali content is higher than in the other femic mineral; K and Na show preference for hornblende over plagioclase (see 219.46 m, 219.3 m, 219.25 m and 217.48 m, Tables 6 and 7).

Plagioclase (Table 7) with An percentages ranging from 94 to 99, is extremely calcic with practically no K_2O. The rocks at 219.15 m, 218.08 m and 217.48 m contain up to 50% plagioclase and the rocks themselves are extremely rich in CaO.

Analyses of *magnetite* are given in Table 8. Total iron was analyzed as Fe_2O_3; Fe^{+2} and Fe^{+3} were calculated assuming ideal stoichiometry. Compositions range from chromiferous magnetite in the lherzolite to nearly pure magnetite in the clinopyroxene-plagioclase rocks. Chrome is concentrated in the magnetite, very little being present in the silicate phases.

In Figure 9, magnetite is plotted against depth in the cores. Cr, Al and Mg vary slightly from cycle to cycle. Within each cycle, Cr and Al both trend inversely to calculated Fe^{+3}; a similar relationship can be seen between Fe^{+2} and Mg.

Table 6

Electron microprobe analyses and unit cell contents of amphibole in samples selected from DDH C4

	Cycle 1			Cycle 2		Cycle 3							Cycle 9		
Depth in metres	225·86	224·94	224·33	224·18	222·81	221·74	220·68	220·09	219·46	219·30	219·25	217·48	188·67	189·45	186·08
SiO_2	53·92	56·82	54·37	57·54	55·54	54·48	53·92	54·32	48·90	47·18	47·12	47·99	54·45	57·35	50·07
TiO_2	0·24	0·08	0·20	0·07	0·05	0·18	0·29	0·28	0·91	0·88	0·84	0·50	0·32	0·14	0·55
Al_2O_3	4·53	2·29	4·83	0·96	2·50	5·00	4·71	4·73	12·79	12·55	10·05	10·24	4·67	0·84	6·73
Cr_2O_3	0·30	0·08	0·24	0·09	0·04	0·26	0·35	0·14	0·04	0·04	0·05	0·01	0·13	0·23	0·25
FeO†	4·79	3·92	4·51	3·76	4·11	4·60	5·32	5·56	7·86	8·80	12·49	11·41	4·62	2·81	5·04
MnO	0·14	0·16	0·15	0·17	0·30	0·17	0·15	0·14	0·45	0·41	0·42	0·52	0·19	0·14	0·16
NiO	0·11	0·04	0·15	0·10	0·06	0·12	0·23	0·18	0·09	0·01	0·06	0·08	0·17	0·19	0·09
MgO	21·38	22·52	21·25	21·84	21·87	21·63	20·59	20·26	16·12	16·01	14·74	14·26	19·73	23·55	22·71
CaO	13·71	14·33	13·53	14·26	14·39	13·01	13·95	14·00	11·73	12·88	12·97	14·01	14·42	14·59	13·32
N_2O	N.D.	0·22	0·50	0·18	0·33	0·65	0·89	0·74	1·43	1·59	1·30	1·09	0·91	0·24	1·34
K_2O	0·03	0·04	0·33	0·04	N.D.	0·31	0·28	0·19	0·31	0·39	0·34	0·34	0·52	0·05	0·52
Total	99·15	100·50	100·06	99·01	99·19	100·41	100·68	100·54	103·63	100·79	100·38	100·45	100·13	100·13	100·81
Number of ions on the basis of 23 oxygens															
Si	7·410	7·669	7·407	7·860	7·616	7·394	7·361	7·414	6·721	6·569	6·709	6·789	7·453	7·746	6·880
Al^{iv}	·590	·331	·593	·140	·384	·606	·030	·586	1·279	1·431	1·291	1·211	·547	·134	1·091
Al^{vi}	·146	·034	·184	·014	·020	·195	·639	·141	·795	·630	·397	·499	·207		
Ti	·025	·008	·021	·030	·005	·018	·119	·029	·113	·920	·090	·053	·033	·014	·057
Fe	·551	·443	·515	·429	·471	·522	·607	·632	·904	1·039	1·487	1·369	·529	·317	·580
Cr	·033	·008	·026	·010	·005	·028	·038	·015	·004	·005	·008	·001	·015	·024	·027
Mn	·017	·007	·017	·020	·035	·020	·017	·016	·052	·049	·051	·062	·022	·016	·019
Ni	·012	·004	·016	·011	·007	·013	·025	·020	·010	·001	·007	·009	·019	·020	·010
Mg	4·380	4·529	4·320	4·446	4·474	4·375	4·190	4·121	3·302	3·322	3·130	3·007	4·025	4·740	4·657
Ca	2·019	2·072	1·978	2·087	2·114	1·892	2·041	2·047	1·728	1·922	1·979	2·123	2·115	2·112	1·961
Na	....	·057	·133	·048	·087	·171	·236	·195	·382	·430	·360	·299	·242	·063	·357
K	·005	·064	·056	·007	....	·054	·049	·033	·055	·069	·062	·061	·091	·008	·091
Mg	63·1	64·3	63·4	63·8	63·4	64·4	61·3	60·6	55·7	52·9	47·5	46·3	60·4	67·1	64·7
Fe	7·8	6·3	7·6	6·2	6·7	7·7	8·9	9·3	15·2	16·5	22·5	21·1	7·9	3·0	8·1
Ca	29·1	29·4	29·0	30·0	29·9	27·9	29·8	30·1	29·1	30·6	30·0	32·6	31·7	29·9	27·2
Mg/(Mg + Fe)	·888	·911	·894	·912	·905	·893	·874	·867	·785	·762	·678	·687	·884	·937	·889
Fe/(Fe + Mg)	·112	·089	·107	·088	·095	·107	·127	·133	·215	·238	·322	·313	·116	·063	·111
Fe/Mg	·126	·098	·119	·970	·105	·119	·145	·153	·274	·313	·475	·455	·131	·067	·125

† All iron as FeO

Analyst: W. R. Morgan, W.A.I.T.

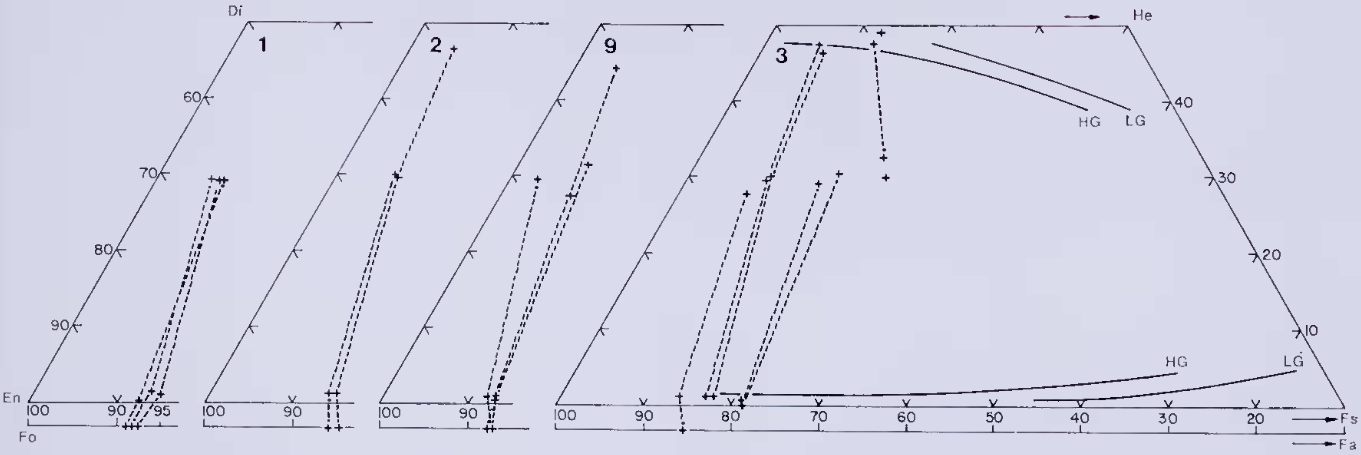

Figure 7.—Composite Ca-Mg-Fe diagram on which the Kondinin pyroxenes, amphiboles, and olivines are plotted. 1, 2, 9, 3 refer to cycles. HG: "higher grade" and LG: "lower grade" pyroxenes of Quairading and Broken Hill.

Table 7

Electron microprobe analyses and unit cell contents of plagioclase in samples selected from DDH C4

	Cycle 3				
Depth in metres	219·46	219·30	219·25	218·08	217·48
SiO_2	43·24	43·17	43·50	43·28	43·09
Al_2O_3	36·62	35·79	35·98	36·22	36·50
Fe_2O_3*	0·35	0·46	0·22	0·43	0·41
MgO	N.D.	0·10	0·11	0·12	0·07
CaO	20·24	19·74	19·81	20·00	20·49
Na_2O	0·42	0·61	0·49	N.D.	0·35
K_2O	0·02	0·02	0·01	0·01	N.D.
Total	100·83	99·24	99·66	100·10	100·94
Number of ions on the basis of 32 oxygens					
Si	7·964	8·029	8·058	8·019	7·944
Al	7·955	7·852	7·862	6·967	7·939
Fe	·049	·064	·030	·060	·057
Mg	....	·028	·030	·032	·019
Ca	3·994	3·934	3·932	3·970	4·172
Na	·151	·219	·176	....	·124
K	·004	·005	·002	·002	....
An	96·3	94·6	95·7	99·9	97·0
Ab	3·6	5·3	4·3	....	3·0
Or	0·1	0·1	....	0·1	....

*All iron as Fe_2O_3. Analyst, W. R. Morgan

Temperature-pressure estimate

Temperature

Temperature estimates, using the method of Wood and Banno (1973) were calculated for the four pyroxene pairs in the lherzolite and its associated rocks. These are listed in Table 10. Compared with the granulite-facies pyroxenes given by Hewins (1975), which include the Quairading pyroxene pairs (Davidson 1968), the data of Jayawardena and Carswell (1976), the estimates are high, and range between 856°C and 1034°C. These data support the evidence of igneous equilibration modified by a metamorphic environment.

Pressure

Mineralogically, the Kondinin rocks have the following assemblages:

Olivine + orthopyroxene + tremolite ± clinopyroxene
Orthopyroxene + hornblende + plagioclase
Hornblende + plagioclase + clinopyroxene ± orthopyroxene
Clinopyroxene + plagioclase ± hornblende

The rocks clearly fall into the plagioclase-peridotite facies. From this, and using the range of temperatures referred to above, together with O'Hara's (1967) pressure-temperature grid, pressure is estimated as less than 6 kb. This is in agreement with an estimate of 3-6 kb made from Herzberg's (1978) clinopyroxene alumina solubility grid of the lherzolite facies, using the data of samples 281.08 m and 217.48 m (Table 5). Obata's (1976) calculations on the solubility of alumina in orthopyroxene suggests pressures of less than 8 kb (from samples 219.47 m and 219.30 m; Table 4).

Discussion

Evidence of igneous emplacement

Petrographically, the lherzolite and its associated plagioclase-bearing rocks show a rhythmic cyclic modal variation with no reversals. The bulk rock chemistry of the lherzolite samples is tholeiitic rather than komatiitic. In Figure 10 Al_2O_3 is plotted against $(FeO + Fe_2O_3)/(FeO + Fe_2O_3 + MgO)$; Archaean tholeiitic and komatiitic rocks occupy sharply defined fields (Naldrett and Cabri 1976). In this diagram, the Kondinin rocks trend from lherzolite in the tholeiitic field to hornblende and clinopyroxene-plagioclase rocks in the komatiite field, showing an enrichment in Al prior to Fe-enrichment. This is, in fact, due to the amphiboles becoming more aluminous prior to their enrichment in Fe.

The cyclic rhythm from olivine-rich to olivine-poor rocks indicates that the lherzolite was emplaced by repeated pulses of magma with some crystallization and crystal settling after each injection. Because none of the cycles shows a complete differentiation series it follows that magma must also have been expelled from the chamber at the same time as crystallization, in the manner proposed by Mathison (1967) for the Somerset Dam intrusion, Queensland.

Table 8

Electron microprobe analyses and unit cell contents of magnetite in samples selected from DDH C4

	Cycle 1			Cycle 2			Cycle 3							Cycle 9		
Depth in metres	225·86	224·94	224·33	224·18	222·81	221·74	220·68	220·09	219·46	219·30	219·25	218·08	217·48	188·67	187·45	186·08
Al_2O_3	1·12	0·74	0·36	1·63	1·15	2·05	2·96	2·19	4·52	1·46	1·50	0·14	0·14	1·77	1·56	1·84
Cr_2O_3	7·18	3·32	4·23	5·95	3·08	9·17	8·57	10·09	0·14	0·11	0·20	0·38	0·50	6·88	7·28	6·76
Fe_2O_3	59·74	64·63	63·34	59·16	62·67	57·99	56·55	53·89	61·95	65·21	66·09	67·05	66·27	58·90	59·03	59·50
FeO*	28·97	28·97	29·31	28·45	28·54	27·39	27·51	29·05	28·08	28·70	29·37	29·13	28·99	28·43	28·45	28·50
MgO	0·78	0·81	0·44	0·81	0·70	2·07	1·91	0·46	1·51	0·59	0·46	0·36	N.D.	1·06	1·10	1·22
Total	97·79	98·47	97·68	95·19	96·14	98·67	97·50	95·68	96·20	96·07	97·62	97·06	95·90	97·04	97·42	97·82

Number of ions on the basis of 32 oxygens

Al	·405	·267	·131	·599	·419	·722	1·052	·276	1·626	·539	·545	·051	·052	·641	·563	·661
Cr	1·741	·802	1·036	1·465	·754	2·168	2·043	2·551	·033	·028	·049	·094	·113	1·672	1·763	1·626
Fe^{+3}	13·783	14·868	14·759	13·864	14·587	13·049	12·828	12·967	14·227	15·362	15·337	15·781	15·826	13·613	13·602	13·628
Fe^{+2}*	7·505	7·481	7·665	7·487	7·459	6·918	7·008	7·849	7·237	7·589	7·649	7·699	7·771	7·379	7·359	7·327
Mg	·359	·371	·205	·380	·327	·931	·868	·221	·695	·277	·213	·169	....	·491	·507	·560

* FeO and Fe^{+2} calculated, assuming ideal stoichiometry. Analyst: W. R. Morgan, W.A.I.T.

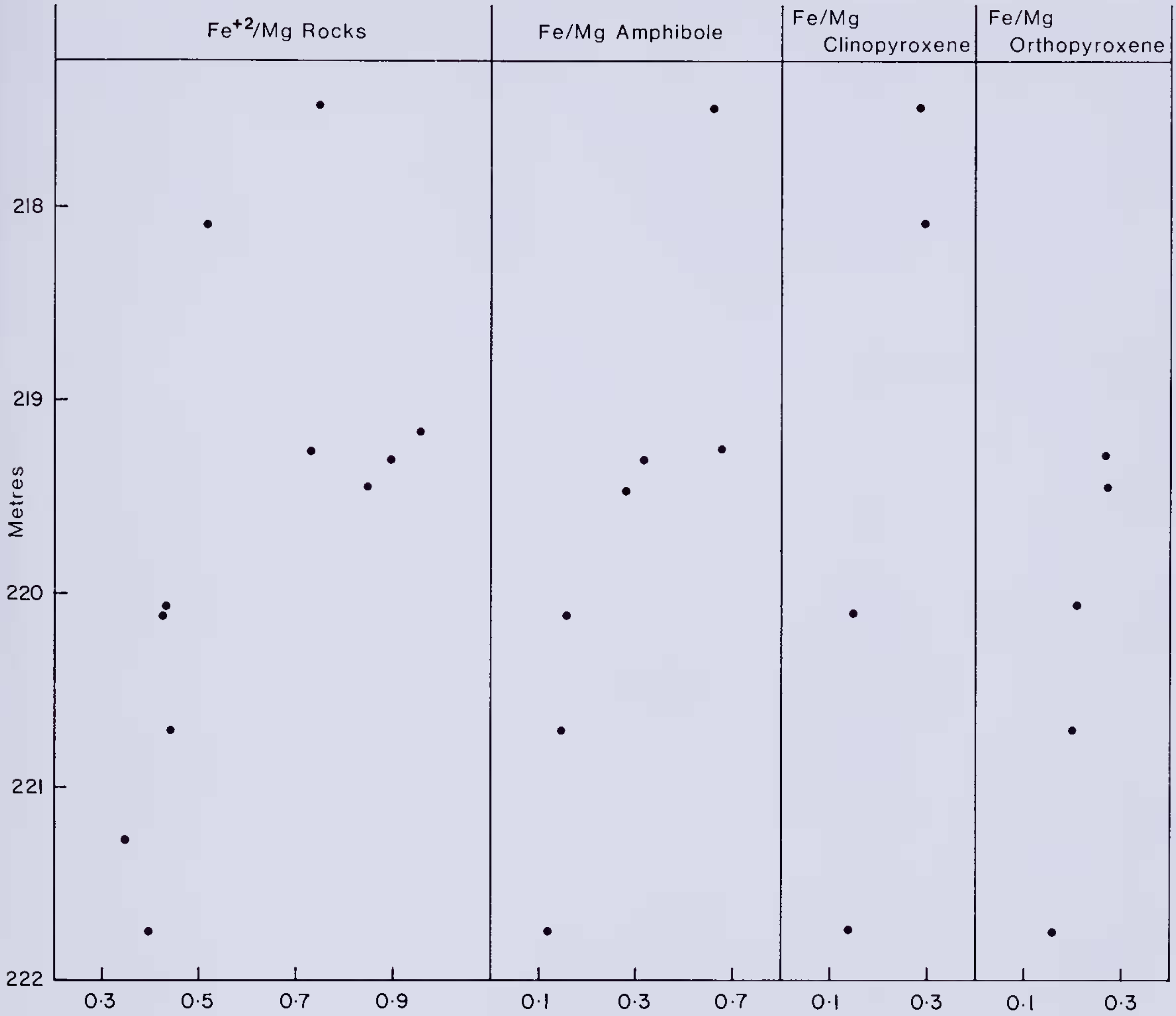

Figure 8.—Cycle 3: The Fe/Mg ratios of rocks, amphiboles, clinopyroxenes, and orthopyroxenes plotted against depth.

Table 9

Fe-Mg distribution coefficients in samples selected from DDH C4

	Cycle 1			Cycle 2		Cycle 3						Cycle 3		
Depth in metres	225·86	224·94	224·33	224·18	222·81	221·74	220·68	220·09	219·46	219·30	217·48	188·67	187·45	186·08
$K_D \frac{\text{Fe/Mg opx}}{\text{Fe/Mg amph}}$	1·1	1·6	1·4	1·7	1·6	1·3	1·4	1·4	1·0	0·8	....	1·1	2·7	1·1
$K_D \frac{\text{Fe/Mg opx}}{\text{Fe/Mg ol}}$	1·1	1·2	1·2	1·0	0·9	1·0	....	....	....	....	....	1·0	0·9	1·0
$K_D \frac{\text{Fe/Mg opx}}{\text{Fe/Mg cpx}}$	....	....	....	....	1·6	....	1·5	1·4	....	....	....	....	....	1·6
$K_D \frac{\text{Fe/Mg ol}}{\text{Fe/Mg amph}}$	1·0	1·4	1·2	1·7	1·7	1·4	....	....	....	....	....	1·1	2·2	1·5
$K_D \frac{\text{Fe/Mg opx}}{\text{Fe/Mg amph}}$	....	....	....	....	1·0	....	....	1·0	....	....	0·6	....	....	0·7

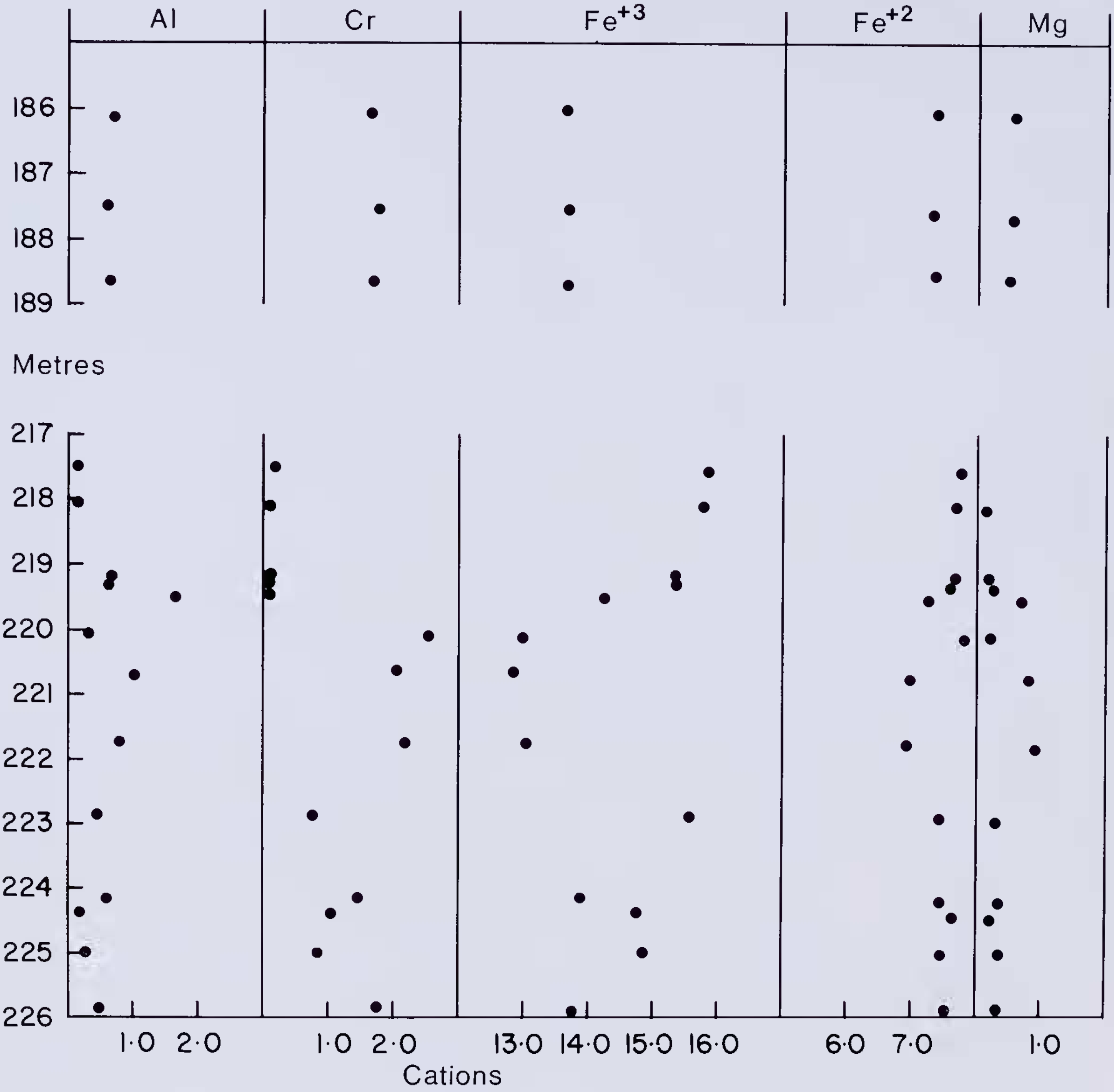

Figure 9.—Compositional variation of magnetite with depth in DDH C4.

Table 10

Temperature estimates (Samples from DDH C4)

Depth in metres	Cycle	Temperature
222·81	2	976°C
220·68	2	856°C
220·09	3	965°C
186·08	9	1034°C

Evidence of metamorphism

The time of emplacement of the ultramafic in relation to the stages of tectonism and metamorphism of the surrounding gneisses is hard to assess. The rocks have crystalloblastic textures and their mineralogy suggests a granulite-amphibolite transition equilibrium perhaps at a slightly lower grade than the mafic gneisses surrounding the body. Figure 1 shows a general lensoid outline of the body, as delineated by the magnetic anomaly; it is elongated parallel to the regional strike as though the body represents a large block tectonically emplaced within the gneisses. These factors would suggest that the ultramafic body, including the lherzolite, was emplaced prior to the tectonism and metamorphism affecting the gneisses.

On the other hand, other features suggest post-tectonic emplacement of the ultramafic. Thus in spite of their crystalloblastic textures the lherzolite and associated rocks show no foliation, tectonite

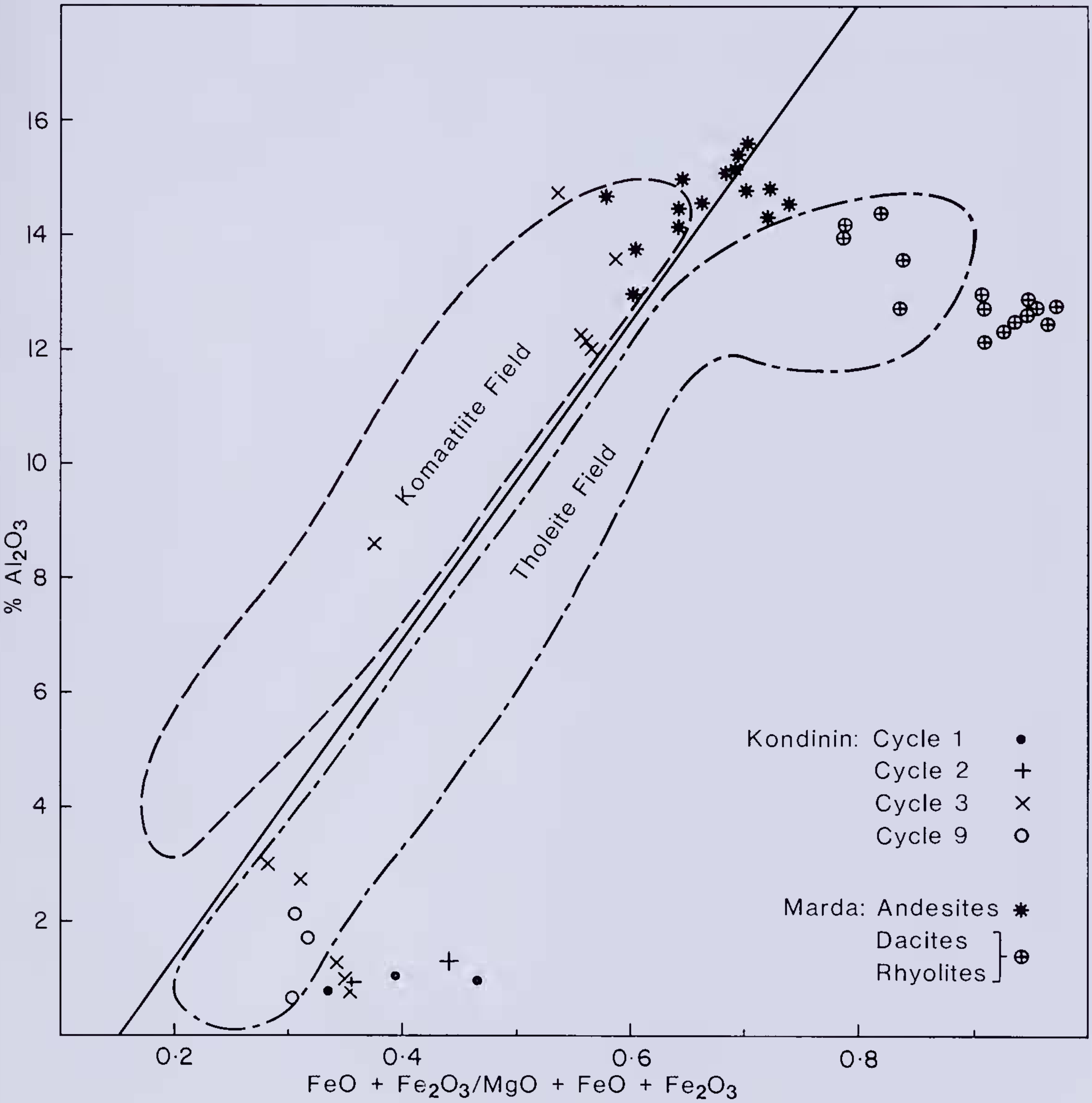

Figure 10.—Plot of Al_2O_3 against $(FeO + Fe_2O_3)/(MgO + FeO + Fe_2O_3)$, after Naldrett & Cabri (1976). Dashed lines: komatiite field. Chain dash line: tholeiite field. Kondinin rocks: • cycle 1; + cycle 2; x cycle 3; o cycle 9. Marda Volcanics (after Hallberg, *et al*, 1976 b) * andesite; + dacite and rhyolite.

fabric or kinking of grains. In addition the orthopyroxene megacrysts of the harzburgite unit referred to earlier are increasingly deformed in the more northerly drill holes but are not deformed in DDH C3 at the south-west corner of the body. At this location, if the ultramafic body was emplaced as a tectonic block, one would expect more extreme deformation of the megacrysts here than further north. The megacryst is more likely to be a relict primary structure due to emplacement of the harzburgite as an igneous intrusion (Morgan, in prep.).

Electron Microprobe X-ray imagery (Fig. 11) of magnetite in the lherzolite shows no zoning of Fe and Cr. Thus there has not been reaction of the magnetite with surrounding silicate phases, as reported by Bliss and MacLean (1975) in chromites from metamorphosed ultramafics in Canada. Indeed, although the Kondinin rocks are enclosed within granulite facies metamorphics, it is evident from the analyses (Table 8) that the magnetite is not of spinel composition; Mg and Al are extremely low even in the hornblendic and plagioclase-bearing rocks

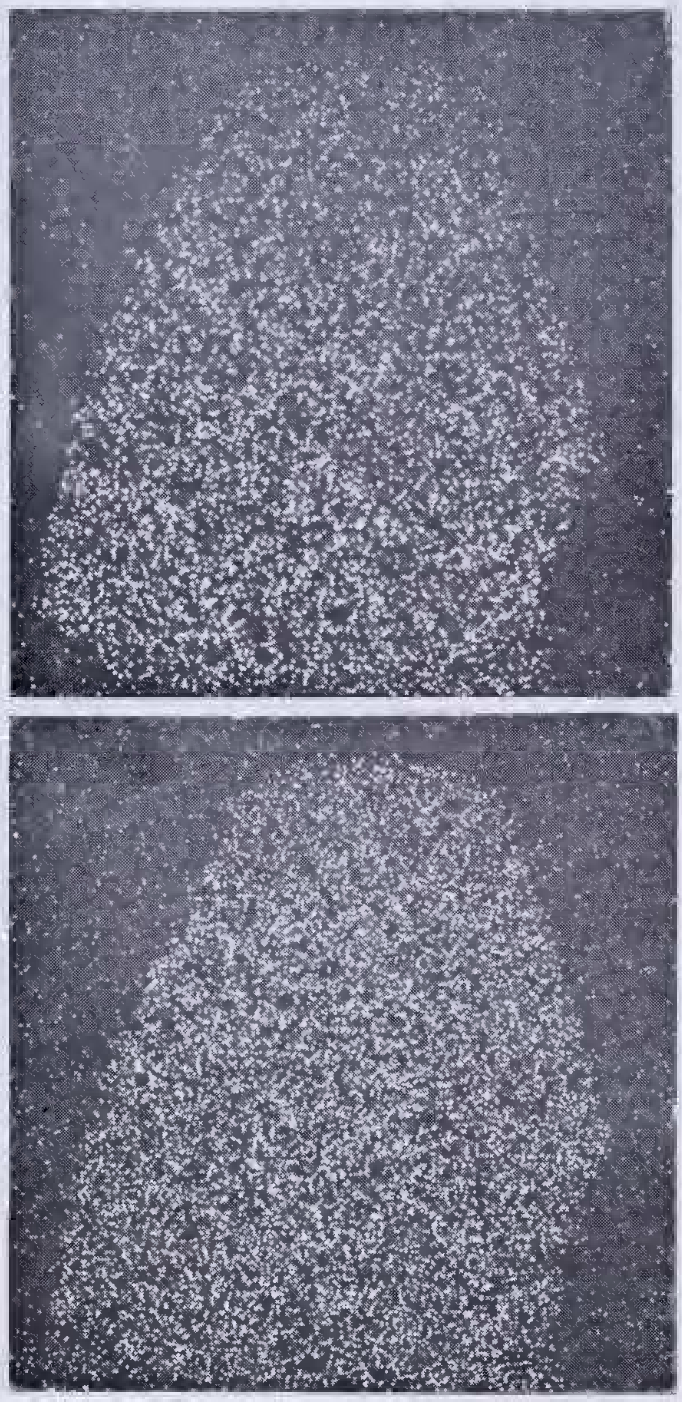

Figure 11.—Electron probe micrographs of a magnetite grain from 225.86 m. (DDH C4), showing lack of zonation in (top) Fe and (bottom) Cr. The grain is approximately 0.5 mm in diameter.

of cycle 3. Evans and Frost (1975) described progressive compositional changes in chrome spinel with increasing metamorphic grade in ultramafic rocks from magnetite to MgAl-spinel. Hence, the lack of zoning and the low Mg and Al support the possibility that the magnetite formed by magmatic crystallization rather than by metamorphic recrystallization.

Thus the evidence suggests that the ultramafic was emplaced during the waning stages of the metamorphism perhaps after the tectonism.

Tentative petrogenesis

If this postulate is correct the repetitive injection, crystallization and expulsion of magma would have taken place during waning metamorphism. Calciferous amphibole crystallized and recrystallized from co-existing pyroxenes and olivine. In cycle 3, the hornblende and thus the rocks are strongly iron-enriched, possibly because hornblende was crystallizing in an amphibolite-granulite environment.

The two samples at 219.47 m and 219.30 m each contain about 50% hornblende. At 219.25 m there is 75% hornblende (Fig. 3). In the hornblende, and the rocks containing them, the Fe/Mg ratios rise sharply up the hole. If the hornblende results from magmatic crystallization, then it would have controlled the Fe/Mg ratio of the remaining liquid perhaps producing calc-alkaline magma, as suggested by the experimental work of Green and Ringwood (1967, 1968). Perhaps we have preserved here a magma chamber into which tholeiitic magma was being repeatedly intruded and from which differentiated tholeiite-like magma and even calc-alkaline liquids were expelled. With the latter in mind, Archaean calc-alkaline volcanics from the Marda Complex, Western Australia (Hallberg *et al.* 1976) have been plotted on Figure 10. Hallberg *et al.* believe the volcanics to be of Andean type (Miyashiro 1974; Morgan 1974) derived from the base of the Archaean crust. If there is any significance in Figure 10 it is the continuance of a "trend" from the Kondinin hornblende and clinopyroxene plagioclase rocks to the Marda andesites and rhyolites.

The fact that the analysed cycles have slightly different modal and chemical compositions suggests the arrival of batches of magma of slightly differing compositions, each batch cooling and settling crystals prior to expulsion of residual magma. Following from this we may imagine that this body represents just one of a plexus of staging places for such magma, with slight differentiation taking place at each stop.

Acknowledgements.—The author is indebted to the Electrolytic Zinc Co. of Australasia for the use of the diamond drill cores which form the basis of this study. Ken and Bet Summers, formerly of Electrolytic Zinc, and Dr. N. Walsh are thanked for their discussions during this work. I am grateful to Professor R. T. Prider, Dr. L. R. Davidson, and Dr. B. F. Windley for their critical review of the manuscript; to Mrs. Coral Green who typed (and retyped) the manuscript; to Mr. Colin Steele who drafted the diagrams; and to J. Lauridson for advice with the microprobe. The paper is published with the permission of the Electrolytic Zinc Co. of Australasia.

References

Anhaeusser, C. R. (1971).—Cyclic volcanicity and sedimentation in the evolutionary development of Archaean greenstone belts of shield areas. *Geol. Soc. Aust., Spec. Publ.* **3**: 57-70.

Binns, A. R. (1962).—Metamorphic pyroxenes from the Broken Hill District, New South Wales. *Mineral. Mag.*, **33**: 320-338.

Bliss, N. W. and MacLean, W. H. (1975).—The paragenesis of zoned chromite from central Manitoba. *Geochim. Cosmochim. Acta*, **39**: 973-990.

Bowes, D. R., Wright, R. E. and Park, R. G. (1964).—Layered intrusive rocks in the Lewisian of the north-west Highlands of Scotland. *Quart. J. Geol. Soc. Lond.*, **120**: 153-191.

Boyd, F. R., Fujii, T. and Danchin, R. V. (1976).—A non-inflected geotherm for the Udachnaya Kimberlite pipe, U.S.S.R. *Carnegie Inst. Washington Year Book*, **75**: 523-531.

Challis, G. A. (1965).—The origin of New Zealand ultramafic intrusions. *J. Petrol.*, **6**: 322-364.

Davidson, L. R. (1968).—Variation in ferrous iron-magnesium distribution coefficients of metamorphic pyroxenes from Quairading, Western Australia. *Contr. Mineral. Petrol.*, **19**: 238-259.

Davidson, L. R. (1971).—Metamorphic hornblendes from basic granulites of the Quairading district, Western Australia. *N. Jb. Miner. Mh. Jg.* 1971 **H8**: 344-359.

Davidson, L. R. and Mathison, C. I. (1973).—Manganiferous orthopyroxenes and garnets from metamorphosed iron formations of the Quairading district, Western Australia. *N. Jb. Miner. Mh. Jg.* 1973 **H2**: 47-57.

Davidson, L. R. and Mathison, C. I. (1974).—Aluminous orthopyroxenes and associated cordierites, garnets, and biotites from granulites of the Quairading district, Western Australia. *N. Jb. Miner. Jg.* 1974 **H6**: 272-286.

Davies, F. B. (1974).—A layered basic complex in the Lewisian, south of Loch Laxford, Sutherland. *J. Geol. Soc. Lond.*, **130**: 279-284.

Donaldson, M. J. (1974).—Petrology of the Munni Munni Complex, Roebourne, Western Australia. *J. Geol. Soc. Aust.*, **21**: 1-16.

Evans, B. W. and Frost, R. B. (1975).—Chrome-spinel in progressive metamorphism—a preliminary analysis. *Geochim. Cosmochim. Acta*, **39**: 959-972.

Frost, R. B. (1975).—Contact metamorphism of serpentinite, chloritic blackwall and rodingite at Paddy-Go-Easy Pass, Central Cascades, Washington. *J. Petrol.*, **16**: 272-313.

Goode, A. D. T. and Moore, A. C. (1975).—High pressure crystallization of the Ewarara, Kalka and Gosse Pile intrusions, Giles Complex, Central Australia. *Contrib. Mineral Petrol.*, **51**: 77-97.

Green, D. H. (1964).—The petrogenesis of the high-temperature peridotite intrusion in the Lizard area, Cornwall. *J. Petrol.*, **5**: 134-188.

Green, T. H. and Ringwood, A. E. (1967).—Crystallization of basalt and andesite under high pressure hydrous conditions. *Earth Planet. Sci. Letters*, **3**: 481-489.

Green, T. H. and Ringwood, A. E. (1968).—Genesis of the calc-alkaline igneous rock suite. *Contr. Mineral. Petrol.*, **18**: 105-162.

Hallberg, J. A. (1972).—Geochemistry of Archaean volcanic belts in the Eastern Goldfields region of Western Australia. *J. Petrol.*, **13**: 45-56.

Hallberg, J. A., Carter, D. N. and West, K. N. (1976a).—Archaean volcanism and sedimentation near Meekatharra, Western Australia. *Precambrian Res.*, **3**: 577-599.

Hallberg, J. A., Johnstone, C. and Bye, S. M. (1976b).—The Archaean Marda igneous complex, Western Australia. *Precambrian Res.*, **3**: 111-136.

Hallberg, J. A. and Williams, D. A. C. (1972).—Archaean mafic and ultramafic rock associations in the Eastern Goldfields region of Western Australia. *Earth Planet. Sci. Letters*, **15**: 191-200.

Herzberg, C. T. (1978).—Pyroxene geothermometry and geobarometry: experimental and thermodynamic evaluation of some subsolidus phase relations involving pyroxenes in the system CaO—MgO—Al_2O_3—SiO_2. *Geochim. Comoschim. Acta*, **42**: 945-957.

Hewins, R. H. (1975).—Pyroxene geothermometry of some granulite facies rocks. *Contrib. Mineral. Petrol.*, **50**: 205-209.

Jacques, A. L. (1976).—An Archaean tholeiitic layered sill from Mt. Kilkenny, Western Australia. *J. Geol. Soc. Aust.*, **23**: 157-168.

Jayawardena, D. E. de S. and Carswell, D. A. (1976).—The geochemistry of "charnockites" and their constituent ferromagnesian minerals from the Precambrian of south-east Sri Lanka (Ceylon). *Mineral. Mag.*, **40**: 541-554.

McCall, G. J. H. and Leishman, J. (1971).—Clues to the origin of Archaean eugeosynclinal peridotites and the nature of serpentinization. *Geol. Soc. Aust., Spec. Pub.* 3: 271-300.

McIver, J. R. (1975).—Aspects of high-magesia eruptives in South Africa. *Contrib. Mineral Petrol.*, **51**: 99-118.

Mathison, C. I. (1967).—The Somerset Dam layered basic intrusion, Southern Queensland. *J. Geol. Soc. Aust.*, **14**: 57-86.

Miyashiro, A. (1974).—Volcanic rock series in island arcs and active continental margins. *Amer. J. Sci.*, **274**: 321-355.

Morgan, W. R. (1974).—A Carboniferous continental andesite-rhyolite association from the "Nychum" area, North Queensland, Australia. *J. Petrol.*, **15**: 97-112.

Morgan, W. R. (1977).—A view of Archaean magmatism. *Mining & Metall. Bull. C. Inst. Mining Metall. Eng. (Taiwan)*, **21**: 100-114.

Naldrett, A. J. and Cabri, L. J. (1976).—Ultramafic and related rocks: Their classification and genesis with special reference to the concentration of nickel sulphides and platinum-group elements. *Econ. Geol.*, **71**: 1131-1158.

Naldrett, A. J. and Mason, G. D. (1968).—Contrasting Archaean ultramafic igneous bodies in Dundonald and Clergue Townships, Ontario. *Can. J. Earth Sci.*, **5**: 111-143.

Nesbitt, R. W. (1971).—Skeletal crystal forms in ultramafic rocks of the Yilgarn Block, Western Australia, evidence for an Archaean ultramafic liquid. *Geol. Soc. Aust., Spec. Publ.* 3: 331-347.

Nesbitt, R. W. and Sun, S-S (1976).—Geochemistry of Archaean spinifex-textured peridotites and magnesian and low-magnesian tholeiites. *Earth Planet. Sci. Letters*, **31**: 433-453.

Obata, M. (1976).—The solubility of Al_2O_3 in orthopyroxene in spinel and plagioclase peridotites and spinel pyroxenite. *Amer. Mineralogist*, **61**: 804-816.

Phillips, F. C. (1971).—The use of stereographic projection in structural geology. Edward Arnold, 3rd Ed.

O'Hara, M. J. (1961).—Zoned ultrabasic and basic gneiss masses in the early Lewisian metomorphic complex at Scourie, Sutherland. *J. Petrol.*, **2**: 248-276.

O'Hara, M. J. (1965).—Ultrabasic and basic gneiss masses in the Lewisian. *Geol. Mag.*, **102**: 296-313.

O'Hara, M. J. (1967).—Mineral facies in ultrabasic rocks, ... *in*: Wyllie, P. J. (ed.), Ultramafic and related rocks, Wiley, 7-18.

Prider, R. T. (1945).—Charnockitic and related cordierite-bearing rocks from Dangin, Western Australia. *Geol. Mag.*, **82**: 145-172.

Purvis, A. C. Nesbitt, R. W. and Hallberg. J. A. (1972).—The geology of part of the Carr Boyd Rocks Complex and its associated nickel mineralization, Western Australia. *Econ. Geol.*, **67**: 1093-1113.

Pyke, D. R., Naldrett, A. J. and Eckstrand, O. R. (1973).—Archaean ultramafic flows in Munro Township, Ontario. *Geol. Soc. Amer. Bull.*, **84**: 955-978.

Varne, R. (1977).—The origin of spinel lherzolite inclusions in basaltic rocks from Tasmania and elsewhere. *J. Petrol.*, **18**: 1-23.

Viljoen, R. P. and Viljoen, M. J. (1971).—The geological and geochemical evolution of the Onverwacht Volcanic Group of the Barberton Mountainland, South Africa. *Geol. Soc. Aust., Spec. Publ.* 3: 133-150.

White, A. J. R., Jakes, P. and Christie, D. M. (1971).—Composition of greenstones and the hypothesis of sea-floor spreading in the Archaean. *Geol. Soc. Aust., Spec. Publ.* **3**: 47-56.

Williams, D. A. C. and Hallberg, J. A. (1973).—Archaean layered intrusions of the Eastern Goldfields region, Western Australia. *Contr. Mineral Petrol.*, **38**: 45-70.

Wilson, A. F. (1971).—Some geochemical aspects of the sapphirine-bearing pyroxenites and related highly metamorphosed rocks from the Archaean ultramafic belt of South Quairading, Western Australia. *Geol. Soc. Aust., Spec. Publ.* 3: 401-412.

Wilson, A. F. and Green, D. C. (1971).—The use of oxygen isotopes for geothermometry of Proterozoic and Archaean granulites. *Geol. Soc. Aust., Spec. Publ.* 3: 389-400.

Wilson, D. D. B., Kilburn, L. C., Graham, A. R. and Ramlal, K. (1969).—Geochemistry of some Canadian nickeliferous ultrabasic intrusions. *Econ. Geol. Monogr.*, **4**: 294-309.

Windley, B. F. (1977).—Layered igneous complexes in Archaean high-grade belts. *Abstracts Vol., Archaean Igneous Geochem. Meeting, Hyderabad.*

Winkler, H. G. F. (1967).—Petrogenesis of metamorphic rocks. Springer-Verlag, New York, 2nd Ed.

Wood, B. J. and Banno, S. (1973).—Garnet-orthopyroxene and orthopyroxene-clinopyroxene relationships in simple and complex systems. *Contr. Mineral. Petrol.*, **42**: 109-124.